Snail hosts abundance mediates the effects of antagonist interactions between trematodes on the transmission of human schistosomes.

Philippe Douchet

philippe.douchet@univ-perp.fr

IHPE: Interactions Hotes-Pathogenes-Environnements   https://orcid.org/0000-0002-6689-1710

Bart Haegeman
UMR7621: Laboratoire d'Oceanographie Microbienne

Jean-François Allienne
IHPE: Interactions Hotes-Pathogenes-Environnements

Jérôme Boissier
IHPE: Interactions Hotes-Pathogenes-Environnements

Bruno Senghor
IRD: Institut de recherche pour le developpement

Olivier Rey
IHPE: Interactions Hotes-Pathogenes-Environnements

---

1   Snail hosts abundance mediates the effects of antagonist interactions

2   between trematodes on the transmission of human schistosomes.

3

4   **Philippe Douchet [1], Bart Haegeman [2], Jean-François Allienne[1], Jérôme Boissier [1], Bruno Senghor [3],**

5   **Olivier Rey [1]**

6

7   **Contact Informations:**

8   [1] IHPE, Univ Montpellier, CNRS, IFREMER, Univ Perpignan Via Domitia, Montpellier, France

9   [2] CNRS/Sorbonne Université, UMR7621, Laboratoire d'Océanographie Microbienne, Banyuls-surMer,

10   France

11   [3] IRD, campus UCAD-IRD de Hann, CP 18524, BP 1386 Dakar, Senegal

12

13   **Corresponding author** : **Olivier Rey :** olivier.rey@univ-perp.fr

14   **Other co-author : Philippe Douchet : philippe.douchet@univ-perp.fr**

15   **Bart Haegeman : bart.haegeman@cnrs.fr**

16   **Jean-François Allienne : jean-francois.allienne@univ-perp.fr**

17   **Jérôme Boissier : boissier@univ-perp.fr**

18   **Bruno Senghor : bruno.senghor@yahoo.fr**

19

20   **<u>Declarations</u>**

23   **Ethics approval and consent to participate**

24   The project has received approval from the National Ethical Committee (CNERS) of Senegal (agree-

25   ment number: 00061/MSAS/CNERS/SP).

Consent for publication

27   "Not applicable"

Availability of data and materials

29   All data generated or analysed during this study are included in this published article [and its supple-

30   mentary information files].

31   This project obtained from the Nagoya office in Senegal, an exemption from authorization of access

32   and use of genetic resources (number: 001339 of November 15, 2021, reference: V/L du 28 octobre

33   2021) by the Competent National Authority (Directorate of National Parks of Senegal).

Competing interests

35   The authors declare that they have no competing interests

Authors' contributions

46   **PD** have made substantial contributions to the conception, design of the work, acquisition,

47   analysis, and interpretation of data. He was a major contributor in writing the manuscript, have

48   approved the submitted version, and have agreed both to be personally accountable for the author's

49   own contributions and to ensure that questions related to the accuracy or integrity of any part of the

50   work, even ones in which the author was not personally involved, are appropriately investigated,

51   resolved, and the resolution documented in the literature.

52   **BH** have made substantial contributions to the creation of the mathematical model used in the work,

53   the analysis, and interpretation of data. He was a major contributor in writing the manuscript, have

54   approved the submitted version, and have agreed both to be personally accountable for the author's

55   own contributions and to ensure that questions related to the accuracy or integrity of any part of the

56   work, even ones in which the author was not personally involved, are appropriately investigated,

57   resolved, and the resolution documented in the literature.

58   **JFA** have made substantial contributions to the acquisition of the molecular data. He have approved

59   the submitted version, and have agreed both to be personally accountable for the author's own

60   contributions and to ensure that questions related to the accuracy or integrity of any part of the work,

61   even ones in which the author was not personally involved, are appropriately investigated, resolved,

62   and the resolution documented in the literature.

63   **JB** have made substantial contributions to the conception, design of the work,

64   acquisition, and interpretation of data. He have approved the submitted version, and have agreed both

65   to be personally accountable for the author's own contributions and to ensure that questions related

66   to the accuracy or integrity of any part of the work, even ones in which the author was not personally

67   involved, are appropriately investigated, resolved, and the resolution documented in the literature.

68   **BS** have made substantial contributions to the acquisition of the field data. He have approved the

69   submitted version, and have agreed both to be personally accountable for the author's own

70   contributions and to ensure that questions related to the accuracy or integrity of any part of the work,

71   even ones in which the author was not personally involved, are appropriately investigated, resolved,

72   and the resolution documented in the literature.

73   **OR** have made substantial contributions to the conception, design of the work, acquisition,

74   and interpretation of data. He was a major contributor in writing the manuscript, have approved the

75   submitted version, and have agreed both to be personally accountable for the author's own

76   contributions and to ensure that questions related to the accuracy or integrity of any part of the work,

77   even ones in which the author was not personally involved, are appropriately investigated, resolved,

78   and the resolution documented in the literature.

86

90

91   1. Abstract (350 mots MAX)

92   **Background:**

93   Combating infectious diseases and halting biodiversity loss are intertwined challenges crucial to ensure

94   global health. Biodiversity can constrain the spread of vector-borne pathogens circulation,

95   necessitating a deeper understanding of ecological mechanisms underlying this pattern. Our study

96   evaluates the relative importance of biodiversity and the abundance of *Bulinus truncatus*, a major

97   intermediate host for the trematode *Schistosoma haematobium* on the circulation of this human

98   pathogen at aquatic transmission sites.

99   **Methods:** We combined mathematical modelling and a molecular based empirical study to specifically

100   assess the effect of co-infections between *S. haematobium* and other trematodes within their *B.*

101   *truncatus* snail hosts; and *B. truncatus* abundance at transmission sites, on the production of *S.*

102   *haematobium* infective cercariae stages released into the aquatic environment.

103   **Results:**

104   Our modelling approach shows that more competitive trematode species exploiting *B. truncatus* as an

105   intermediate host at the transmission site level leads to higher co-infection rates within snail hosts,

106   subsequently reducing the production of *S. haematobium* cercariae. Conversely, an increase in *B.*

107   *truncatus* abundance results in lower co-infection rates, and a higher proportion of *S. haematobium*

108   cercariae released into the environment. Our empirical data from the field support these findings,

109   indicating a significant negative effect of local trematode species richness and co-infection rates on the

110   dominance of S. *haematobium*, while *B. truncatus* abundance positively influences *S. haematobium*

111   dominance.

112   **Conclusions:**

113   Our study highlights the importance of biodiversity in influencing the transmission of *S. haematobium*

114   through the effect of antagonistic interactions between trematodes within bulinid snail hosts. This

115   effect intensifies when *B. truncatus* populations are low, promoting co-infections within snails. In line

116   with the need for concrete applications of the One Health concept, we advocate for maintaining high

117   global freshwater biodiversity to sustain global trematode diversity at transmission sites, offering a

118   cost-effective means to significantly reduce schistosome prevalence and intensity while preserving

119   aquatic ecosystem services.

120

121

122   ## 2. Introduction

123   One of the major consequences of global change is a drastic modification of the circulation of

124   pathogens and an increase in disease emergences and outbreaks worldwide (1–3). The causes of these

125   global-scale increases are multifactorial and the profound changes in biodiversity observed globally

126   contribute significantly (4). On one hand, while some populations/species are extending, including

humans and all domesticated species upon which human societies rely, most populations of most

species are declining (5,6). On the other hand, it is generally assumed that parasite transmission

increases with host density although generally not linearly (7). As a result, the growth and densification

of human populations and domestic organisms contribute to the emergence and circulation of

numerous pathogens sometimes causing severe health and economic issues which tend to extend at a

planetary scale due to global international trades (8). Moreover, the reduction in biodiversity in an

existing community of hosts and parasites can lead to a decrease in the abundance of non-competent

hosts, which, when present, mitigate the circulation of parasites through a dilution effect (9). The

generality and ecological importance of this dilution effect is however widely debated (10–12).

Additionally, host diversity in a community can support the co-existence of several circulating pathogen

species, between which antagonistic (or beneficial) interactions within their hosts or vectors can

significantly hamper (or facilitate) the circulation of least competitive pathogens (13).

Both facilitating and antagonistic interactions exist between trematodes. These parasitic

worms display complex life cycles more generally including a vertebrate organism as definitive hosts

and several successive invertebrate and/or vertebrate organisms are intermediate hosts including most

of the time (aquatic) snails as first intermediate hosts. Such complex life cycles provide opportunities

for interactions between trematode species and modulation of their transmission dynamics when

coinfection occur especially in snail species that generally serve as amplifiers of trematodes in the

environment. Some trematodes are causative agents of severe forms of Human and livestock diseases

such as *Schistosoma* species. Interactions between *Schistosoma* species and other trematodes were

historically documented with a focus on antagonistic interactions that could hamper their transmission

as a mean of potential biological control strategies (14).

In fact, accruing evidence suggest that *Schistosoma* species that develop into sporocysts within their

snail hosts are considered as moderate to bad competitors compared to other trematode species (13).

Moreover, other trematode species that develop into rediae within snail hosts can predate the co-

occuring *Schistosoma* sporocysts under development while consuming snail tissues (15). At natural

153 transmission sites of *Schistosoma* species, the importance of such antagonist interactions on the

154 circulation of *Schistosoma* species is generally underappreciated. Importantly however the snail

155 intermediate hosts used by some *Schistosoma* species (e.g. *Biomphalaria spp.*, *Bulinus spp.*) generally

156 host numerous trematode species hence providing opportunities for many intra-host interactions that

157 involve *Schistosoma* species. For example, up to 29 trematode species have been identified in natural

158 populations of *Biomphalaria pfeifferi* and *Biomphalaria sudanica* established over a constrained

159 geographical scale, these two snail species being important hosts for *Schistosoma mansoni* in eastern

160 Africa (13). Moreover, and as previously mentioned, *Schistosoma* species harbor low competitiveness

161 compared to many other species of trematodes (13). In line with these two characteristics, recent

162 modelling approaches predict over 50% decrease in the transmission of *S. mansoni* in the presence of

163 some highly competitive trematodes coinfecting *B. pfeifferi* – such as *Calicophoron sukari*, a widely

164 distributed parasite across livestock (13).

165   As a simple baseline, the prevalence of coinfection in a host population harbouring two

166 parasites equals the product of the prevalence of single infection of each parasite in the population

167 (15). However, coinfection rates observed *in natura* are generally lower than this theoretical

168 expectation. Interspecific competition leading to the rapid exclusion of one interacting species,

169 recruitment heterogeneity either due to random or parasite behaviours that limit co-infections,

170 immune priming mechanisms and high cost of co-infection on hosts fitness, may explain the departure

171 of this theoretical expectation as generally observed *in natura* (15,16). Intriguingly, the effect of host

172 abundance on co-infection rates is generally neglected since this theoretical expectation relies on the

173 relative prevalence of co-infection, which corresponds to the proportion of hosts that are infected (or

174 co-infected) among all hosts present in the environment. However, according to the generally

175 acknowledged density-dependent nature of pathogen transmission, it is expected that host density

176 also influences the co-infection rates, the occurrence of antagonistic interactions and ultimately the

177 transmission of less competitive parasites. If so, this could constitute an additional indirect mechanism

178   by which host density is positively correlated with parasite transmission by reducing co-infections and

179   a release from antagonistic interactions.

180   Using the *Schistosoma haematobium – Bulinus truncatus* system as a model, the objective of

181   this study is to assess the relative importance of the density of *B. truncatus* at transmission sites and

182   the diversity of trematodes that use *B. truncatus* on the risk of transmission of *S. haematobium*.

183   *Schistosoma haematobium* is a trematode species causing the urogenital form of bilharziasis in Humans

184   mainly in the tropical regions in Africa (17). It displays a complex two-host lifecycle that involves

185   humans as vertebrate hosts, in which the adults develop and reproduce sexually resulting in the

186   production of thousands of eggs that are released in the environment through the urinary system of

187   the host; and *Bulinus truncatus*, a freshwater snail host in which the parasite reproduce asexually

188   resulting in the production of cercariae that are released in the aquatic environment and actively seek

189   and penetrate the skin of a new vertebrate definitive host.

190   We hypothesise that for a given abundance of *B. truncatus*, an increase in the specific richness

191   of trematodes using *B. truncatus* as a host at the community scale would lead to an increase in co-

192   infection rates that involves *S. haematobium*. Given that *Schistosoma* species (including *S.*

193   *haematobium*) tend to be moderate competitors, an increase in the rate of co-infection is expected to

194   reduce the development of *S. haematobium* within their snail hosts and so the total amount of *S.*

195   *haematobium* cercariae released from the snails into the aquatic environment and ultimately the risk

196   of transmission to their definitive hosts. Moreover, an increase in the abundance of *B. truncatus* would

197   lead to a reduction of the co-infection rates and the associated antagonistic interactions thus ultimately

198   enhancing the risks of schistosomiasis transmission to Humans.

199   To test these hypotheses, we first built a simple mathematical model to describe (i) how the

200   number of competitive trematodes using *B. truncatus* influence the amount of *S. haematobium*

201   cercariae released in aquatic systems and (ii) how snail density (here carrying capacity) influences co-

202   infections rates and the associated antagonistic effects on the release of *S. haematobium* cercariae at

203   the transmission site level. We confronted this mathematical model to an empirical field work study

204 conducted in Northern Senegal at 9 previously identified urogenital schistosomiasis transmission sites.

205 We combined traditional malacological and parasitological approaches and next-generation molecular

206 tools to empirically study the effect of the trematodofauna using *B. truncatus* as intermediate host and

207 the local abundance of *B. truncatus* on the transmission of *S. haematobium*.

208

209

3. Material and methods

3.1. Mathematical model

2.1.1.Model with one trematode species

213 We start by modelling the infection of a snail population by a single trematode species. The

214 model tracks the dynamics of the density of miracidia, susceptible and infected snails, and cercariae in

215 the aquatic ecosystem, denoted by the variable $M(t)$, $S(t)$, $I(t)$ and $C(t)$ respectively. The dynamics are

216 described by the following set of ordinary differential equation :

$$
\begin{aligned}
\frac{\mathrm{d}M}{\mathrm{d}t} &= g - eSM - d_M M \\
\frac{\mathrm{d}S}{\mathrm{d}t} &= -eSM - d_S S + f_S S\left(1 - \frac{S+I}{K}\right) \\
\frac{\mathrm{d}I}{\mathrm{d}t} &= eSM - d_I I + f_I I\left(1 - \frac{S+I}{K}\right) \\
\frac{\mathrm{d}C}{\mathrm{d}t} &= sI - d_C C - uC
\end{aligned}
$$

217 These equations use the following parameters: g : input rate of miracidia; e : infection rate of

218 susceptible snails by miracidia ; f_S, f_I : fitness of susceptible and infected snails; K : carrying capacity of

219 snail population; s : shedding rate of infected snails; u : uptake rate of cercariae by mammals; d_M, d_S, d_I

220 , d_C : loss rates of miracidia, susceptible snails, infected snails, cercariae. Because infection reduces

221 fitness and increases mortality, $f_I < f_S$ and $d_I > d_S$. For simplicity we set $f_I = 0$ and $d_S = 0$. Note that the

222 model does not describe the complete trematode life cycle. Rather, the model starts from a given

223 exposure to miracidia (parameter g) and predicts the cercariae density (variable C), or equivalently the

224 uptake of cercariae by mammal hosts (equal to uC). To simplify the study of the model, we look at its

225 equilibrium properties (Additional _File_1_(Figure_S1)).

2.1.2.Model with two trematode species

228   Next, we consider two trematode species infecting a snail population. We call these two species

229   *1* and *2*. Compared to the previous model, we extend the list of variables as follows: miracidia M_1 and

230   M_2, susceptible S, infected I_1, I_2 and co-infected I_{12}, and cercariae C_1 and C_2. The equations are :

$$\frac{\mathrm{d}M_1}{\mathrm{d}t} = g_1 - e_1 S M_1 - d_{M_1} M_1$$

$$\frac{\mathrm{d}M_2}{\mathrm{d}t} = g_2 - e_2 S M_2 - d_{M_2} M_2$$

$$\frac{\mathrm{d}S}{\mathrm{d}t} = -e_1 S M_1 - e_2 S M_2 + f_S S\Big(1 - \frac{S + \sum I}{K}\Big)$$

$$\frac{\mathrm{d}I_1}{\mathrm{d}t} = e_1 S M_1 - e_2 I_1 M_2 - d_{I_1} I_1$$

$$\frac{\mathrm{d}I_2}{\mathrm{d}t} = e_2 S M_2 - e_1 I_2 M_1 - d_{I_2} I_2$$

$$\frac{\mathrm{d}I_{12}}{\mathrm{d}t} = e_2 I_1 M_2 + e_1 I_2 M_1 - d_{I_{12}} I_{12}$$

$$\frac{\mathrm{d}C_1}{\mathrm{d}t} = s_1 I_1 + s_{1|2} I_{12} - d_{C_1} C_1 - u_1 C_1$$

$$\frac{\mathrm{d}C_2}{\mathrm{d}t} = s_2 I_2 + s_{2|1} I_{12} - d_{C_2} C_2 - u_2 C_2$$

231   The meaning of the model parameters is as before, but now with the indices *1* and *2* referring to the

232   trematode species. For the shedding rates, s_1 is the shedding rate of cercariae of species *1* by a snail

233   infected by species *1* only, whereas $s_{1|2}$ is the shedding rate of cercariae of species *1* by a snail infected

234   by both species. Similar definitions hold for s_2 and $s_{2|1}$. We assume that the two trematode species only

235   differ in their shedding rates. The term "shedding" used in the model reflect the transition from the

236   day when snails become infected to the release of cercariae, and hence also includes the development

237   of the trematodes within the snail hosts. Taking species *1* as a *Schistosoma* species, we model its

238   inferior competitivity by taking $s_{1|2} < s_{2|1}$ (i.e., co-infected snails preferentially shed cercariae of species

239   *2*). For simplicity, we set $s_{1|2} = 0$ and $s_{2|1} = s_2$. In other words, snails that are infected by both species do

240   not shed *Schistosoma* cercariae, and they shed cercariae of the other species at the same rate as a snail

241   not co-infected by *Schistosoma*. Apart from this difference in shedding rates, we assume the two

242   trematode   species   to   be   equivalent   for   all   other   model   parameters   (Additional

243   _File_2_&_3_(Figure_S2_and_S3)).

244

2.1.3.Model with multiple trematode species

246   The above model can be extended to more than two trematode species. We denote by n the

247   number of trematode species, and assume that snails can be infected by one, two, . . . , all n species.

248   We make the same assumptions as above, that is, all trematode species are assumed to be equivalent

249   apart from their shedding rates. In particular, we consider one *Schistosoma* species and n−1 other

250   trematode species and assume that there is no shedding of *Schistosoma* cercariae in case snails are co-

251   infected with (one or more) other trematode species. We assume that the miracidia input rate per

252   trematode species is independent of diversity, so that the total input rate (i.e., summed over all

253   trematode species) increases proportionally with diversity. In particular, the input rate of *Schistosoma*

254   miracidia is unaffected by the presence of other trematode species. We assume that the total shedding

255   rate (i.e., the shedding rate per infected snail and summed over all shedded trematode species) is

256   independent of the number of species infecting the snail. This implies that the shedding rate per snail

257   infected by a particular trematode species decreases with trematode diversity, as some of these snails

258   are co-infected with other trematode species. This holds especially for snails infected by *Schistosoma*,

259   as co-infection by another trematode species causes the *Schistosoma* shedding rate to drop to zero. An

260   additional file provides an in-depth description of the model equations and our simulations

261   (Additional_File_4_(Supplementary_material), Additional_File_5_&_6)

262

3.2. Empirical field work

263

2.2.1.Study sites description and ethical consideration

264

265   An empirical fieldwork study was carried out in the region of the Senegal river basin during the

266   dry season in February 2022 (Figure 1). We targeted 9 previously identified *S. haematobium*

267   transmission sites that differ from an ecological point of view (i.e. river, irrigation canal and lake) and

268   hence possibly harbouring different trematode communities. Each of these transmission sites is close

269   to a village where the prevalence and intensity of urogenital schistosomiasis among children was

270   previously reported (18).

271   The transmission sites close to the villages of Ndiawara (16°35′04″N / 14°50′58″W), Ouali Diala

272   (16°35′56″N / 14°56′10″W), Dioundou (16°35′50″N / 14°53′22″W), Fonde Ass (16°36′20″N /

273   14°57′38″W) and Khodit (16°35′45″N / 14°56′42″W) are located in the middle valley along a tributary

274   of the Senegal River ("le Doue" river). The transmission site close to the village of Guia (16°35′51″N /

275   14°55′31″W) is located along an irrigation canal that drains water from the river "le Doue". The

276   transmission sites nearby the villages of Mbane (16°16'15"N / 15°48'7"W) and Saneinte (16°14'32"N /

277   15°48'6"W) are located along the east shore of the lake de Guiers. The transmission site close to the

278   village of Lampsar (16°6'34"N / 16°20'58"W) is in an inlet in the lower valley of the Senegal river delta

279   (Figure 1).

280

281   *2.2.2.eDNA, snails and trematodes field sampling*

282   To assess the abundance of *B. truncatus* and to identify all trematode species present at each

283   of the 9 studied sites as free-living stages, aquatic environmental DNA samples (eDNA) were collected

284   using water filter capsules according to Douchet et al. (2022). Filtrations were carried out from the

285   entire water column along the banks until the filter's membrane clogged, and the volume filtered at

286   each site was recorded. At each site but Khodit, 1.5L of commercial spring water was filtered following

287   the same protocol as a technical field negative control. Once the water filtrations completed, capsules

288   were drained, filled with 50 mL of Longmire buffer solution to preserve eDNAs, vigorously shaken, and

289   stored at room temperature and at dark until subsequent DNA extraction.

290   Once the eDNA sampling achieved, all snails found at each sampling site were systematically

291   collected manually or by scooping the grass on the water bench using a colander for about 30 minutes

292   to one hour. Snails were morphologically identified and individualized on well plates filled with

293   dechlorinated water and left to emit trematodes for 2 h in the afternoon under natural sunlight.

294   Cercariae from each emitting snail were collected and transferred onto FTA cards and stored at room

295   temperature until DNA extraction and molecular identification. Coupled with eDNA samples, this

296   approach allows a better characterisation of the trematode community at each transmission site and a

297   quantification of the prevalence of each emitted trematode species among the locally established snail

298   populations including *Bulinus truncatus*. All snails morphologically identified as *B. truncatus* (either

299   emitting or non-emitting) were preserved individually in alcohol until DNA extraction. Subsequent

300   molecular analyses aimed at validating the species attribution of each *B. truncatus* individual, check for

301   the presence and identification of potentially developing trematodes within each snail, refine measures

302   of prevalence of each trematode species, and identify possible coinfections.

303

304   3.3. Experimental infection

305   Twenty six non-emitting snails (although possibly naturally infected by trematodes) sampled at

306   sites Guia, Fonde Ass, Khodit and Saneinte were kept alive and individually exposed to 3   *S.*

307   *haematobium* miracidia for 2 hours in 24 well plates filled with dechlorinated water. The miracidia used

308   for this experimental mollusc exposition were from a homogenised pool of *S. haematobium* eggs of

309   eight children from the Lampsar village provided by the Sen_Hybrid_Invasion project. The 104 exposed

310   snails (i.e. 26 x 4) were maintained and fed *ad libitum* for a period of 1 month and survival was checked

311   daily. At the end of this period, the infection status of each *B. truncatus* was monitored by emission of

312   cercariae once a week until the snails died. To this end, *B. truncatus* were individualized on clean well

313   plates filled with dechlorinated water and stimulated to emit trematodes for 4 h in the afternoon under

314   artificial light. Cercariae released from emitting snails were collected and stored at -20°C until DNA

315   extraction for subsequent molecular identification. All along the experiment, each emitting snail was

316   kept individualised to identify possible trematode species emission shifts through time. At the end of

317   the experiment, all *B. truncatus* individuals (either emitting or non-emitting) were preserved in alcohol

318   individually until DNA extraction.

319

3.4. Molecular approaches

2.4.1. DNA extractions from samples

To extract eDNAs from water filtrates, the Longmire solution contained in each capsule was poured into three 50 ml Falcon tubes as technical replicates. For the field negative controls (i.e. Spring water filtrates), each capsule content was recovered in one 50 ml Falcon tube only. All Falcon tubes were centrifugated at 16,000 g for 20 min and the supernatant was removed. We then collected 0.25 g to 0.5 g of sediment from the pellet from each falcon tube or 500 µL of Longmire remaining at the base of the falcon tube when not enough material was observed. For negative controls, 500 µl of Longmire were systematically retained when discarding the supernatant. This pre-extraction step led to the processing of 35 samples (i.e., 8 negative controls and 3 extraction replicates for each of the 9 environmental samples). Total environmental genomic DNA was extracted from each triplicate and negative controls using the Qiagen's Dneasy PowerSoil Pro Kit following supplier recommendation performing the physical lysis with a MagNA Lyser at a speed of 7,000 for 30s.

DNAs from all cercariae obtained from the field survey, from the exposure experiment and from all *B. truncatus* snails were extracted using the Qiagen DNeasy Blood & Tissue kit. Regarding cercariae preserved onto FTA cards, we manually isolated 0.5 cm in diameter pieces containing the biological material using a sterile punch and placed them in 1.5 ml tubes. Four samples consisting in 0.5 cm in diameter pieces from cards on which ultrapure water had been deposited were also isolated as DNA extraction negative controls. For cercariae preserved in 1.5 ml tubes stored at -20°C, we thawed the tubes and centrifuged them at 20,000g for 10 minutes before removing the supernatant. To obtain extraction and PCR negative controls, we also centrifuged 2 tubes that contained ultrapure water following the same protocol. For *B. truncatus*, we first rinsed the snails with tap water and ground them entirely and individually with a sterile pestle in 1.5 mL tubes. To obtain extraction and PCR negative controls, we also processed 7 assuredly non-infected *B. truncatus* from our laboratory collections in the same way. Moreover, 3 extraction/PCR positive controls were prepared from 3 additional non-infected laboratory *B. truncatus* individuals, to which one *S. haematobium* cercariae from our

346 laboratory collections was artificially added before DNA extraction processing. These pre-extraction

347 steps led to the processing of 328 samples and 16 controls (i.e., 29 FTA card pieces and 4 associated

348 negative controls, 28 cercaria preserved in alcohol and 2 associated negative controls and 281 *B.*

349 *truncatus* including 173 *B. truncatus* from the field and 98 from the experimental infection and 3 and

350 7 associated positive and negative controls). From these samples, we then followed the Tissue protocol

351 as recommended by the supplier applying a 2 h lysis for cercariae and an overnight lysis for snails.

352

353 *2.4.2. Taxonomical assignment of trematode cercariae by barcoding*

354 To taxonomically assign each cercariae emitted from snail hosts to a trematode species, DNAs

355 extracted from cercariae of each emitting snail were SANGER sequenced at the *28S D2* rDNA gene

356 domain and at the *16S* rDNA gene (19). PCRs were run using the obtained 57 DNAs extracted from

357 cercariae and the 6 negative controls on both markers. PCRs were performed using the GoTaq® G2 Hot

358 Start Polymerase kit of Promega. Each PCR reaction contained Colorless Buffer at 1×, MgCL2 at 1.5 mM,

359 dNTPs at 0.2 mM, primers at 0.4 µM, 1.25 units of GoTaq G2 Hot Start, 2 µl of DNA sample, and

360 ultrapure water for a total PCR reaction volume of 35 µL. For the *28S* marker, the PCR program was

361 used as follows: An initial denaturation step at 94°C for 3' followed by 40 cycles with a denaturation

362 step at 95°C for 30 s, a hybridization step at 56°C for 30 s and an elongation step at 72°C for 30 s. We

363 finally performed a final elongation step at 72°C for 5'. For the *16S* marker, the same PCR program was

364 used, except that 35 cycles were performed, the hybridization temperature was 54°C and the

365 elongation time was 15 s. Ten microliters of the resulting PCR products were migrated on a 2% agarose

366 gel for 20' at 135 V and revealed using a Vilber Infinity 1000 imaging system. Each individual PCR

367 product from the 57 cercariae DNA extracts that displayed an expected theoretical size was then

368 sequenced in both the forward and reverse directions on an ABI 3730xl sequencer at the GenoScreen

369 platform (Lille, France). The sequences generated were aligned, trimmed, and taxonomically assigned

370 with a MEGABLAST analysis for the *28S* and the *16S* markers. For the taxonomical assignment of each

371 cercariae, the common taxonomic rank to all hits above 96% of identity over 97% of coverage were

372 kept.

373

374 *2.4.3.Molecular taxonomic validation of B. truncatus and infection diagnostic*

375 The 271 *Bulinus* spp. sampled in the field from which total DNA was extracted were diagnosed

376 to verify that they belonged to the species *B. truncatus* using a molecular diagnosis by LAMP based on

377 the internal transcribed spacer (ITS2) *B. truncatus* species-specific (20). DNAs extracted from *Bulinus*

378 spp. were first diluted at 1/100e and a negative control consisting in a 1/100e diluted DNA extraction

379 from *Bulinus globosus* was used. Each LAMP reaction contained an Isothermal Amplification Buffer II

380 reaction buffer [20 mM Tris–HCl, 10 mM (NH4)2SO4, 150 mM KCl, 2 mM MgSO4, 0. 1% Tween 20, pH

381 8.8 at 25 °C (New England Biolabs, UK)] at 1X, additional MgSO4 at 3 mM, dNTP at 1.0 mM, internal

382 primers FIP and BIP at 1.2 µM, external primers F3 and B3 at 0.2 µM, LOOP primers LB and LF at 0.4

383 µM, 1 U of Bst 2.0 WarmStart DNA polymerase (New England Biolabs, UK), 1 µl of DNA sample, and

384 ultrapure water for a total reaction volume of 10 µL as described in Blin et al., 2023. Reaction were

385 performed in a thermocycler at 63 °C for 45 min followed by an enzyme inactivation phase at 80 °C for

386 5 min. Result visualizations were done using a final point visual detection of fluorescence after adding

387 1 µl of 1:50 diluted 10,000× concentration of SYBR Green (Invitrogen) (green: positive=*B. truncatus*

388 species; orange: negative=other than *Bulinus* species).

389 To detect trematodes within the tissues of each *B. truncatus*, we used the 16S rDNA gene

390 metabarcode initially developed to characterize trematode communities from eDNA (19) as a

391 molecular diagnostic tool. PCRs were performed using the GoTaq® G2 Hot Start Polymerase kit of

392 Promega following the same PCR condition as described previously [see section 2.4.2], except that

393 reactions were performed in a final volume of 10 µl and using 2 µL of DNA extracted from *Bulinus* spp.

394 diluted 1:100. Amplification success was assessed visually by migrating the ten microliters of the

395 resulting PCR products on a 2% agarose gel for 20' at 135 V and revealed using a Vilber Infinity 1000

396 imaging system.

2.4.4.Trematodes-specific MiSeq sequencing on the infected B. truncatus individuals and on the eDNA to characterize trematode communities

A total of 137 positive *16S* metabarcoding NGS libraries were prepared following the Illumina two-step PCR protocol, using the Trem_16S_F1 and the Trem_16S_R2 primers set up with Illumina adapters using 2 µL of eDNA or DNA extracted from *B. truncatus* diluted at 1:100e as previously described (19). Libraries were sent and paired-end sequenced (2 × 250 bp) on an Illumina MiSeq™ at the BioEnvironnement platform (University of Perpignan Via Domitia, France). Three samples were eliminated from the analyses of the MiSeq sequencing because they did not meet the defined threshold of 25,000 sequences required to normalise samples by rarefaction (i.e., one non emitting *B.truncatus* from the site Ouali Diala, and two PCR duplicates from water eDNA).

2.4.5.Abundance of B. truncatus determination by ddPCR on eDNA

Abundance of *B. truncatus* at each study site was assessed by digital droplet PCR (ddPCR) from eDNA sampled by water filtration according to (21). We first pooled the eDNA extraction triplicates from each of the 9 sampling sites. As negative control, we also pooled DNAs extracts from one individual of each mollusc species sampled during the field work in addition to DNAs extracts from 3 *B. truncatus* sister species (i.e., *B. globosus*, *B. senegalensis* and *B. umbilicatus*) from our laboratory collection. As positive control, we used a DNA extract at 0.01 ng/µL from one *B. truncatus* from our laboratory collection. We ran ddPCRs using the TaqMan technology on a QX200 AutoDG Droplet Digital System (BioRad) at the Bio-environment platform (Perpignan, France). We used the Btco2F (5' ATTTTGACTTTTACCACCAT 3') and Btco2R (5' GATATCCCAGCTAAATGAAG 3') primers combined with the FAM-labelled probe Btco2P (5' TCGAAGGAGGGGTTGGAACAGG-FAM 3'). ddPCR reactions were performed using the BioRad ddPCR Supermix for Probes (No dUTP). Each ddPCR reaction contained the BioRad MIX at 1X, primers at 0.5 µM, probes at 0.25 µM, 7 µL of eDNA template or 2 µL of control DNAs templates, and ultrapure water for a total ddPCR reaction volume of 20 µL. After the droplets

423 generation, the ddPCR program was used as follows: An enzyme activation step at 95°C for 10 min

424 followed by 40 cycles with a denaturation step at 94°C for 30s and an annealing/extension step at 60°C

425 for 60s, with a ramp setting to 2°C/s. We finally performed an enzyme deactivation step at 98°C for 10'.

426 The resulting fluorescence signal were analysed using QuantaSoft software V1.7 (BioRad). A signal was

427 considered positive (i.e., with the presence of *B. truncatus* DNA) if at least one positive droplet was

428 detected and if the positive droplet displayed the same order of fluorescence magnitude as the positive

429 droplet obtained from a ddPCR positive control.

430

431 3.5. Data analysis

432 *2.5.1.Characterisation of trematode communities present in the water and exploiting B.*

433 *truncatus populations*

434 The resulting amplicon sequence datasets from the MiSeq sequencing was processed using the

435 Find Rapidly OTUs with Galaxy Solution (FROGS) (22) according to (19). Briefly, the produced datasets

436 were pre-processed by filtering out the sequences to keep amplicon sizes from 150 to 400 nucleotides.

437 The remaining sequences were next clustered into operational taxonomic units (OTUs) using the swarm

438 algorithm and using denoising and an aggregation distance of three (23). The resulting dataset was

439 filtered out for chimeras using VSEARCH (24). Singletons and underrepresented clusters (i.e., clusters

440 whose number of sequences were <0.1% of the total number of sequences) were removed. Lastly, we

441 conservatively considered that a given OTU was present in a library if its number of sequences was

442 >0.1% of the total number of sequences in this library.

443 Each OTU was next assigned to a taxonomic level (either a species or a genus) using a two-step

444 BLAST affiliation process. The first BLAST analysis was computed using the standalone blastn program

445 contained in the *BLAST+* package and a custom trematode sequence database containing 174

446 sequences (82 sequences from the NCBI database and 92 sequences from a custom internal trematode

447 sequence database including the sequences obtained from the amplicons generated by the SANGER

448 sequencing on cercariae, see section 1.1.7). The second BLAST analysis was performed using the online

449 MEGABLAST tool and based on the nr database without restricting parameters to achieve affiliation of

450 OTUs that could not be assigned in the first BLAST analysis. OTUs were assigned to a species if the

451 sequences presented a minimal blast coverage of 97% and a pairwise identity above 99% with the

452 affiliated sequence. OTUs were assigned to a genus if the sequences presented a minimal blast

453 coverage of 97% and a pairwise identity above 96% with the affiliated sequence. OTUs that could not

454 be assigned to a species or genus were assigned to a higher taxonomic rank using a clustering method

455 based on the pairwise genetic distances between the OTUs and the same set of 174 sequences as

456 above. We then aligned these sequences with T-Coffee on EMBL-EBI (25) and built a neighbor joining

457 phenetic tree based on the percentage of nucleotide differences from the obtained alignment using

458 Jalview version 2.11.1.4 (26) for visualization.

459 Subsequent analyses were then performed on R version 4.3.1. Each library was normalized by

460 rarefaction at 25,000 reads using the package *Vegan* version 2.6-4. The trematode composition, specific

461 richness and relative abundance in each *B. truncatus* individual or water sample was next assessed

462 using the package *phyloseq* (27). We assessed the co-infection rates among infected *B. truncatus* and

463 the number of trematode species involved in each co-infection. We also tested whether parasite

464 aggregation at the *B. truncatus* individual scale occurred by comparing the observed distribution of

465 trematode species within hosts with a theoretical distribution following a negative binomial

466 distribution using a Chi-square test.

467

468 *2.5.2.Abundance of B. truncatus at each sampling site*

469 The *B. truncatus* eDNA copy number per liter of filtered water (C_L) estimated from the ddPCR

470 results was used as a proxy of the abundance of *B. truncatus* at each sampling site. C_L was calculated

471 from the following equation (21):

$$C_L = \frac{\frac{C_{rdd} * V_e}{V_r}}{V_w}$$

472

473   With C_L: the number of eDNA c/L for the amplified sample ; C_{rdd}: the copy number per reaction

474   volume ; V_e: the total volume of eluted DNA after extraction ; V_r: the volume of extracted DNA used for

475   ddPCR reaction ; and V_w: the total volume of filtered water.

476

477   *2.5.3. Assessing the link between the relative abundance of Schistosoma quantified in co-*

478   *infected B. truncatus and the emission status of Schistosoma cercariae by co-infected B.*

479   *truncatus*

480   To determine whether the dominance status of *Schistosoma* species in terms of percentage of

481   reads of these species within *B. truncatus* individuals co-infected with other trematode species can be

482   used as a proxy of *Schistosoma* cercarial release, we performed a generalised linear model (GLM) using

483   the package *stats* version 4.3.1 implemented in R. A subset from our dataset that contained 14 *B.*

484   *truncatus* individuals from the field work and from the experimental infection were used for this

485   analysis. These individuals were all emitters, co-infected and harboured at least *S. haematobium* or *S.*

486   *bovis*. We set the emission status (i.e. 0 and 1: non-emitting and emitting *Schistosoma sp.*) as the

487   dependent variable and the relative abundance of the respective *Schistosoma* species in terms of

488   percentage of sequences compared to the other co-infecting trematode species as explanatory

489   variable. The model was built assuming a quasibinomial distribution of the data.

490

491   *2.5.4. Effect of trematode species richness, co-infection rates and host abundance on the*

492   *average dominance of schistosomes*

493   To test our initial hypotheses, we ran three independent generalized linear mixed models

494   (GLMM) using the package *lme4* version 1.1-33 implemented in R to infer the effect of (i) the overall

495   trematode species richness using *B. truncatus* as an intermediate host at the population level, (ii) the

496   co-infection rate among the infected *B. truncatus* snails, and (iii) the abundance of *B. truncatus;* on the

497   average dominance of schistosomes within host populations (i.e., the relative abundance of *S.*

498   *haematobium* or *S. bovis* in terms of percentage of sequences compared to the other co-infecting

499   trematode species). Only naturally infected *B. truncatus* from the field were considered in this analysis,

500   excluding *B. truncatus* from the experimental infection. To account for pseudo-replication, we set the

501   sampling site as a random factor. For these analyses, the co-infection rate variable was transformed

502   into two categories (i.e. <50% and >50% co-infection among infected individuals). The *B. truncatus*

503   abundance variable was also transformed into two categories (i.e. <200 and >200 C_L) to compare sites

504   at low and medium to high density according to Mulero et al. 2020. The variable "trematode species

505   richness" (that uses *B. truncatus)* was coded as the number of trematode species other than

506   *Schistosoma* which use local *B. truncatus* population at the site level. We assumed a binomial error

507   term in the three models tested.

508

509

510   ## 4. Results

511   ### 4.1. Mathematical model

512   Our mathematical model indicates that, for a fixed carrying capacity of *B. truncatus* (either

513   small or large), a local increase in the number of competitive trematode species using *B. truncatus* as

514   intermediate host leads to an increase in the co-infection rate within individual snails and ultimately to

515   a decrease in the number of *S. haematobium* cercariae produced (Figure 2). Moreover, an increase of

516   carrying capacity of *B. truncatus* leads to a decrease of the proportion of co-infected snails and an

517   increase in the proportion of *Schistosoma* cercariae (Figure 2). In other words, an increase in the

518   number of competitive trematode species using *B. truncatus* as intermediate host can reduce the

519   production of *S. haematobium* cercariae through antagonist interactions and particularly so when *B.*

520   *truncatus* populations are small. An increase in *B. truncatus* populations mitigates the effect of

521   antagonist interactions by reducing the coinfection rate among snail hosts.

522

4.2. Empirical field study

Except *Bulinus forskalii* that was recorded at low abundance at 3 sites (i.e., Ouali Diala, Guia and Khodit), *B. truncatus* was the only *Bulinus* species found during the field survey. The species identity of the 271 snails initially identified as *B truncatus* based on their morphology, and from which total DNA was extracted, was validated by the LAMP-based diagnostic tool. The abundance of *B. truncatus* among sites assessed based on digital PCRs results varied from 41 to 2176 eDNA copies per litre filtered (Table 1).

In addition to *S. haematobium* and its sister species *S. bovis*, we identified 9 trematode species associated with *B. truncatus* populations. Nine trematode species were sampled during our fieldwork (Figure 3), and two additional trematode species were detected during the monitoring of experimentally infected *B. truncatus* individuals, including *Apharyngostrigea pipientis* and an *Echinostoma* species that we could not determine at the species level (Additional_File_7_(Table S1)). An additional species (i.e. Paramphistomoidea sp. 3) was found associated to two *B. truncatus* individuals from the experimental infection (Additional_File_7_(Table S1)) under the appearance of cysts attached on their shell (despite washing) but with no apparent shedding from snails. The number of trematode species other than S. *haematobium* and *S. bovis* using the *B. truncatus* population at each site varied from 0 to 4 species and the co-infection rates among infected individuals from 0 to 100% (Figure 3; Table 1). The distribution of the number of trematode species per *B. truncatus* individual from the field did not differ significantly from a theoretical negative binomial distribution hence indicating a classical parasite aggregation pattern in *B. truncatus* populations (Additional_File_8_(Figure S4)).

Apart from the *B. truncatus* population, a total of 20 trematode species were detected from the water samples, 7 of which were also detected in *B. truncatus* while 2 trematodes detected in *B. truncatus* were not detected from the water samples. *Schistosoma haematobium* and/or *S. bovis* were detected from eDNA water filtrates at 5 among the 9 targeted sites (Additional_File_9_(Table S2)).

Table 1 : Volume of water filtered, abundance of *B. truncatus*, molecular prevalence of *Schistosoma* in

B. truncatus populations, specific richness of tremadtodes that use *B. truncatus* populations as a host

(other than *Schistosoma*), co-infection rate among infected snails, and average number of reads

attributed to *Schistosoma* among snails infected by *Schistosoma*, per site.

Site	Volume of water filtered (L)	*B. truncatus* abundance (DNA copies / litre of filtered water)	Molecular prevalence of *Schistosoma* in *B. truncatus*	Trematode richness using *B. truncatus* as host other than *schistosoma*	Rate of co-infections among infected individuals	Average % of *Schistosoma* reads in *B. truncatus* individuals infected by *Schistosoma*
Ndiawara	6.5	78	0,0	4	0.33	00.00
Ouali_Diala	10	41	2,3	3	0.83	34.94
Guia_canal	5	61	23,8	3	1.00	20.67
Dioundou	10	75	0,0	0	NA	00.00
Fonde_Ass	10	57	0,0	1	0.00	00.00
Khodit	5	333	29,4	1	0.20	99.74
Mbane	2.8	104	0,0	0	NA	00.00
Saneinte	3.5	2176	8,3	2	0.25	50.15
Lampsar	18	58	6,3	1	0.25	80.63

553

During all the molecular analysis steps, all the negative and positive controls behaved as

expected. The prevalences of trematodes including that of schistosomes in *B. truncatus* populations,

assessed from our molecular diagnostic approach, were higher than the prevalences measured by the

emission method only (Additional_File_10_(Table S3)).

Overall the emitting *B. truncatus* infected by *Schistosoma* species and by at least one other

species of trematode, *Schistosoma* species are shed only when they are dominant in terms of relative

sequenced reads abundance compared to that of the other co-infecting trematode species

(Additional_File_11_(Figure_S5)). Moreover, in all but one case, the haplotype of the trematode

species emitted corresponds to the most abundant haplotype obtained from NGS sequencing in co-

infected *B. truncatus* (Figure 3; Additional_File_7_(Table_S1)).

564   Both the local richness of trematode species exploiting *B. truncatus* population (p-value =

565   0.029; AIC = 14.9) and the coinfection rate (p-value = 0.020, AIC = 17.4) have a significant negative effect

566   on *Schistosoma spp.* dominance based on our GLMM models. Conversely, the local abundance of *B.*

567   *truncatus* positively and significantly affects *Schistosoma spp.* dominance (p-value = 0.047, AIC =20.1).

568   Based on the comparison of AICs obtained from the three statistical models ran, the model accounting

569   for the local richness of trematode species exploiting *B. truncatus* population is the best supported

570   which strengthens the idea that this factor is the most important in explaining *Schistosoma spp.*

571   dominance. At site level, the co-infection rate among infected snails tended to increase when the total

572   trematode species richness exploiting the *B. truncatus* population increased, although the correlation

573   was not significant (Table 1). Conversely, this same co-infection rate tended to decrease when the

574   abundance of *B. truncatus* increased (Table 1).

575

576

577   5. Discussion / Conclusion

578   Understanding the ecological mechanisms that drive the circulation of parasites is primordial

579   to better identify transmission site, better assess transmission risks and guide strategies to fight against

580   parasites and the associated diseases while preserving the integrity of the socio-ecosystem health

581   (28,29). In this context, the ecology of transmission of *Schistosoma* species that are involved in

582   bilharziasis forms associated to humans and to a lesser extent to animals, and the impact of human

583   activities on the circulation of these parasites have received considerable attention and particularly so

584   in the last decade (30,31).

585   The presence and abundance of compatible snail hosts in a given system are determining factors in the

586   establishment and circulation of *Schistosoma* parasites, particularly as they modulate the rate of

587   contact between the parasites released into the system and the hosts (i.e. encounter filter; (32,33)).

588   In the present study we theoretically and empirically show that reducing snail host abundance

589   also hamper the circulation of *S. haematobium* indirectly by promoting snail co-infections with other

590   potentially more competitive trematode species and hence a reduction of *S. haematobium* cercariae

591   produced by local *B. truncatus* populations. This competition effect on the circulation of *S.*

592   *haematobium* becomes negligeable when *B. truncatus* populations are abundant. In other word, the

593   size of local snail host populations for parasites of the genus *Schistosoma* may predict the risk of

594   transmission for definitive vertebrate hosts including humans because it determines not only the

595   encounter filter, but also modulates the 'competence' (*sensu largo*) of the locally established snail hosts

596   by influencing their probability of being co-infected with other competitive trematode species (i.e.

597   compatibility filter; (32,33)). This result is based on the generally acknowledged assumption that

598   *Schistosoma* species are bad to moderate competitors (13,15). Although we could not empirically

599   assess the hierarchical rank of competitive ability of each trematode detected in *B. truncatus*

600   populations during our field survey we can expect that at least some of these outcompete or even

601   predate *S. haematobium*, particularly those known to produce rediae during their intra-mollusc

602   parasitic stage such as *Petasiger* sp.

603   Coinfections are rarely observed in the field which could suggest that the effect of the resulting

604   antagonistic interactions between co-occurring parasites could be of relatively weak importance. We

605   here argue that coinfections are likely to be generally underestimated. In particular, we believe that

606   traditional techniques to detect trematodes that develop within their snail hosts via dissection or

607   induced cercarial emission, might lead to an underestimation of coinfection rates. This might be

608   particularly true when *Schistosoma* species are present in the form of degraded, or even invisible

609   traces, resulting from competition or predation induced by other trematodes species. In this regard,

610   high throughput next generation sequencing approaches such as metabarcoding used in this study

611   appear promising to better assess coinfection rates and overall trematode communities within natural

612   snail host populations (34). These metabarcoding approaches are the 'interspecific equivalent' of the

613   genotyping approaches that have revealed the initially unsuspected intraspecific diversity of parasites

614   within their hosts in the past decades (35–37).

615   Our model also points toward the fact that the intensity of such within-snail host competitive

616   effects on *S. haematobium* cercariae production increases with the number of trematode species using

617   the targeted *B. truncatus* population. This theoretical result is also supported by our empirical study. It

618   is interesting to note that the presence of a single highly competitive trematode species at high

619   abundance at a given transmission site and using a given population of *B. truncatus*, would locally result

620   in a similar decrease in the amount of cercariae of *S. haematobium* co-occurring at this site. In fact,

621   biological control strategies based on the dissemination of farmable competitive trematode species

622   that use snail vectors of parasites of the genus *Schistosoma* at active transmission sites have been

623   proposed in the past (38). However, this situation, if not artificially maintained, is generally uncommon

624   *in natura*. Conversely, several studies, including ours, indicate that parasites of the genus *Schistosoma*

625   naturally cooccur frequently with several trematode species that use *Schistosoma* snail intermediate

626   hosts in the field (13). Since trematode species composition is determined by the composition of

627   vertebrate communities locally established either temporary or permanently (39), maintaining

628   vertebrate host diversity that supports trematode diversity in local snail populations could help to

629   reduce the transmission of *Schistosoma* species. For this effect to be sustainable over time, the

630   trematodes released by their vertebrate definitive hosts must complete their entire life cycle locally,

631   which also implies the maintenance of other compartments of biodiversity, including numerous

632   vertebrates (e.g. fish, amphibians) and invertebrates (e.g. aquatic insects). Unfortunately, our

633   ecological knowledge of most trematodes is sorely lacking, and their life cycles are still poorly

634   documented. Huge works remain to be done to characterise both the fauna involved in supplying

635   trematodes that interact with species of the genus *Schistosoma* in their intermediate hosts, and the

636   fauna involved in maintaining the local life cycles of these trematodes. We believe that the newly

637   available metabarcoding tools such as used in the present study (19,34,40), combined with the

638   implementation of large and well documented sequence datasets, provide a promising avenue to

639   characterise trematode life cycles.

640   Our study suggest that maintaining high levels of biodiversity in freshwater aquatic ecosystems

641   could help reducing the transmission of parasites of the genus *Schistosoma*. Several synergetic effects

642   of biodiversity could reduce the circulation of these parasites (29). For instance, several organisms

643   including fish crustaceans and oligochaetes can predate free-living stages of *Schistosoma* parasites and

644   hence reduce their abundance and therefore the risk of infection for mammals (41). However, the

645   negative effect of local biodiversity on the circulation of *Schistosoma* species is all the greater when

646   host snail populations are small. Eradication of snail populations that host *Schistosoma* species is

647   generally considered as the best alternative to fight against schistosmiasis and is one of the

648   recommendations of the WHO (42). Although this strategy is theoretically efficient at short term, its

649   deployment on a large spatial and temporal scale is questionable for several reasons. First, the

650   molluscicides commonly used and spread into aquatic ecosystems are sometimes poorly accepted by

651   Human communities using these ecosystems for water supply. Second, the effects of molluscicides on

652   the overall biodiversity associated with aquatic environments are still poorly understood (43–46).

653   Finally, while these products are efficient against snail communities established locally, they do not

654   prevent the recolonization of these species after treatment. In this context, and alternatively to the

655   application of chemical-based molluscicide, several environment-based strategies aiming at reducing

656   snail hosts abundance while providing services to local human populations are emerging such as the

657   introduction of edible predators of snail hosts (e.g. crayfish) or the extraction of specific aquatic plants

658   that serve as refuge for aquatic snails to produce compost, (47,48). Combined with massive drug

659   administration campaign in human populations and the application of the WASH protocol (42), these

660   guided sustainable strategies of reduction or eradication of aquatic snail host populations that

661   constitute intermediate hosts for *Schistosoma*, generally lead to an important reduction in the rate of

662   re-infection and prevalence of schistosomiasis in neighbouring human populations (49). We here argue

663   that the implementation of sustainable strategies to preserve the biodiversity associated with aquatic

664   ecosystems could be an additional and potentially low-cost means of significantly reducing the

665   prevalence and intensity of bilharziasis, without necessarily eliminating totally host snail populations.

666 These strategies are in line with the need for concrete applications of the One Health concept,

667 particularly recently applied in the case of aquatic parasites including schistosomes (50), and the

668 objectives established by the WHO to reduce the prevalence and intensity of schistosomes below a

669 threshold below which these diseases can no longer be considered a public health problem (42).

670

671

672 6. Références

673 1. Gottdenker NL, Streicker DG, Faust CL, Carroll CR. Anthropogenic Land Use Change and Infectious
674   Diseases: A Review of the Evidence. EcoHealth. 1 déc 2014;11(4):619-32.

675 2. Jones KE, Patel NG, Levy MA, Storeygard A, Balk D, Gittleman JL, et al. Global trends in emerging
676   infectious diseases. Nature. févr 2008;451(7181):990-3.

677 3. White RJ, Razgour O. Emerging zoonotic diseases originating in mammals: a systematic review of
678   effects of anthropogenic land-use change. Mammal Rev. oct 2020;50(4):336-52.

679 4. Keesing F, Ostfeld RS. Impacts of biodiversity and biodiversity loss on zoonotic diseases. Proc Natl
680   Acad Sci. 27 avr 2021;118(17):e2023540118.

681 5. Bar-On YM, Phillips R, Milo R. The biomass distribution on Earth. Proc Natl Acad Sci. 19 juin
682   2018;115(25):6506-11.

683 6. Ceballos G, Ehrlich PR, Barnosky AD, García A, Pringle RM, Palmer TM. Accelerated modern
684   human–induced species losses: Entering the sixth mass extinction. Sci Adv. 19 juin
685   2015;1(5):e1400253.

686 7. Hopkins SR, Fleming-Davies AE, Belden LK, Wojdak JM. Systematic review of modelling
687   assumptions and empirical evidence: Does parasite transmission increase nonlinearly with host
688   density? Methods Ecol Evol. 2020;11(4):476-86.

689 8. Baker RE, Mahmud AS, Miller IF, Rajeev M, Rasambainarivo F, Rice BL, et al. Infectious disease in
690   an era of global change. Nat Rev Microbiol. avr 2022;20(4):193-205.

691 9. Civitello DJ, Cohen J, Fatima H, Halstead NT, Liriano J, McMahon TA, et al. Biodiversity inhibits
692   parasites: Broad evidence for the dilution effect. Proc Natl Acad Sci. 14 juill
693   2015;112(28):8667-71.

694 10. Halsey S. Defuse the dilution effect debate. Nat Ecol Evol. févr 2019;3(2):145-6.

695 11. McCallum HI. Lose biodiversity, gain disease. Proc Natl Acad Sci. 14 juill 2015;112(28):8523-4.

696 12. Wood CL, Lafferty KD, DeLeo G, Young HS, Hudson PJ, Kuris AM. Does biodiversity protect humans
697   against infectious disease? Ecology. 2014;95(4):817-32.

698   13. Laidemitt MR, Anderson LC, Wearing HJ, Mutuku MW, Mkoji GM, Loker ES. Antagonism between
699   parasites within snail hosts impacts the transmission of human schistosomiasis. eLife. 17 déc
700   2019;8:e50095.

701   14. Jourdane J, Mounkassa JB, Imbert-Establet D. Influence of intramolluscan larval stages of
702   *Echinostoma liei* on the infectivity of *Schistosoma mansoni* cercariae. J Helminthol. mars
703   1990;64(1):71-4.

704   15. Kuris AM, Lafferty KD. COMMUNITY STRUCTURE: Larval Trematodes in Snail Hosts. Annu Rev Ecol
705   Syst. 1994;25(1):189-217.

706   16. Laidemitt MR, Gleichsner AM, Ingram CD, Gay SD, Reinhart EM, Mutuku MW, et al. Host
707   preference of field-derived *Schistosoma mansoni* is influenced by snail host compatibility and
708   infection status. Ecosphere. 2022;13(4):e4004.

709   17. Leger E, Webster JP. Hybridizations within the Genus *Schistosoma*: implications for evolution,
710   epidemiology and control. Parasitology. janv 2017;144(1):65-80.

711   18. Senghor B, Mathieu-Begné E, Rey O, Doucouré S, Sow D, Diop B, et al. Urogenital schistosomiasis
712   in three different water access in the Senegal river basin: prevalence and monitoring praziquantel
713   efficacy and re-infection levels. BMC Infect Dis. 29 déc 2022;22(1):968.

714   19. Douchet P, Boissier J, Mulero S, Ferté H, Doberva M, Allienne J, et al. Make visible the invisible:
715   Optimized development of an environmental DNA metabarcoding tool for the characterization of
716   trematode parasitic communities. Environ DNA. mai 2022;4(3):627-41.

717   20. Blin M, Senghor B, Boissier J, Mulero S, Rey O, Portela J. Development of environmental loop-
718   mediated isothermal amplification (eLAMP) diagnostic tool for *Bulinus truncatus* field detection.
719   Parasit Vectors. 28 févr 2023;16(1):78.

720   21. Mulero S, Boissier J, Allienne JF, Quilichini Y, Foata J, Pointier JP, et al. Environmental DNA for
721   detecting *Bulinus truncatus*: A new environmental surveillance tool for schistosomiasis
722   emergence risk assessment. Environ DNA. 2020;2(2):161-74.

723   22. Escudié F, Auer L, Bernard M, Mariadassou M, Cauquil L, Vidal K, et al. FROGS: Find, Rapidly, OTUs
724   with Galaxy Solution. Bioinformatics. 15 avr 2018;34(8):1287-94.

725   23. Mahé F, Rognes T, Quince C, Vargas C de, Dunthorn M. Swarm: robust and fast clustering method
726   for amplicon-based studies. PeerJ. 25 sept 2014;2:e593.

727   24. Rognes T, Flouri T, Nichols B, Quince C, Mahé F. VSEARCH: a versatile open source tool for
728   metagenomics. PeerJ. 18 oct 2016;4:e2584.

729   25. Madeira F, Park Y mi, Lee J, Buso N, Gur T, Madhusoodanan N, et al. The EMBL-EBI search and
730   sequence analysis tools APIs in 2019. Nucleic Acids Res. 2 juill 2019;47(W1):W636-41.

731   26. Waterhouse AM, Procter JB, Martin DMA, Clamp M, Barton GJ. Jalview Version 2—a multiple
732   sequence alignment editor and analysis workbench. Bioinformatics. 1 mai 2009;25(9):1189-91.

733   27. McMurdie PJ. joey711/phyloseq [Internet]. 2024 [cité 18 mars 2024]. Disponible sur:
734   https://github.com/joey711/phyloseq

735 28. De Garine-Wichatitsky M, Binot A, Ward J, Caron A, Perrotton A, Ross H, et al. "Health in" and
736   "Health of" Social-Ecological Systems: A Practical Framework for the Management of Healthy and
737   Resilient Agricultural and Natural Ecosystems. Front Public Health [Internet]. 2021 [cité 24 août
738   2023];8. Disponible sur: https://www.frontiersin.org/articles/10.3389/fpubh.2020.616328

739 29. Douchet P, Gourbal B, Loker ES, Rey O. *Schistosoma* transmission: scaling-up competence from
740   hosts to ecosystems. Trends Parasitol. juill 2023;39(7):563-74.

741 30. Hoover CM, Rumschlag SL, Strgar L, Arakala A, Gambhir M, Leo GA de, et al. Effects of
742   agrochemical pollution on schistosomiasis transmission: a systematic review and modelling
743   analysis. Lancet Planet Health. 1 juill 2020;4(7):e280-91.

744 31. Shaikh N, Rahman-Shepherd A, Dar O. Schistosomiasis in the Senegal River basin. Lancet Planet
745   Health. 1 mai 2018;2:S27.

746 32. Combes C. Parasitism: The Ecology and Evolution of Intimate Interactions. University of Chicago
747   Press; 2001. 743 p.

748 33. Kincaid-Smith J, Rey O, Toulza E, Berry A, Boissier J. Emerging Schistosomiasis in Europe: A Need
749   to Quantify the Risks. Trends Parasitol. 1 août 2017;33(8):600-9.

750 34. Hammoud C, Mulero S, Van Bocxlaer B, Boissier J, Verschuren D, Albrecht C, et al. Simultaneous
751   genotyping of snails and infecting trematode parasites using high-throughput amplicon
752   sequencing. Mol Ecol Resour. 2022;22(2):567-86.

753 35. Criscione CD, Poulin R, Blouin MS. Molecular ecology of parasites: elucidating ecological and
754   microevolutionary processes. Mol Ecol. 2005;14(8):2247-57.

755 36. Dabo A, Durand P, Morand S, Diakite M, Langand J, Imbert-Establet D, et al. Distribution and
756   genetic diversity of *Schistosoma haematobium* within its bulinid intermediate hosts in Mali. Acta
757   Trop. 24 juin 1997;66(1):15-26.

758 37. Theron A, Sire C, Rognon A, Prugnolle F, Durand P. Molecular ecology of *Schistosoma mansoni*
759   transmission inferred from the genetic composition of larval and adult infrapopulations within
760   intermediate and definitive hosts. Parasitology. nov 2004;129(5):571-85.

761 38. Combes C. Trematodes: antagonism between species and sterilizing effects on snails in biological
762   control. Parasitology. avr 1982;84(4):151-75.

763 39. Hechinger RF, Lafferty KD. Host diversity begets parasite diversity: bird final hosts and trematodes
764   in snail intermediate hosts. Proc R Soc B Biol Sci. 20 mai 2005;272(1567):1059-66.

765 40. Thomas LJ, Milotic M, Vaux F, Poulin R. Lurking in the water: testing eDNA metabarcoding as a
766   tool for ecosystem-wide parasite detection. Parasitology. févr 2022;149(2):261-9.

767 41. Koprivnikar J, Thieltges DW, Johnson PTJ. Consumption of trematode parasite infectious stages:
768   from conceptual synthesis to future research agenda. J Helminthol. janv 2023;97:e33.

769 42. WHO WH. Ending the neglect to attain the sustainable development goals: a road map for
770   neglected tropical diseases 2021–2030. 2020 [cité 7 oct 2023]; Disponible sur:
771   https://policycommons.net/artifacts/538380/ending-the-neglect-to-attain-the-sustainable-
772   development-goals/1515029/

773   43. Andrews P, Thyssen J, Lorke D. The biology and toxicology of molluscicides, bayluscide. Pharmacol
774   Ther. 1 janv 1982;19(2):245-95.

775   44. Dawson VK. Environmental Fate and Effects of the Lampricide Bayluscide: a Review. J Gt Lakes
776   Res. 1 janv 2003;29:475-92.

777   45. King CH, Sutherland LJ, Bertsch D. Systematic Review and Meta-analysis of the Impact of
778   Chemical-Based Mollusciciding for Control of *Schistosoma mansoni* and *S. haematobium*
779   Transmission. PLoS Negl Trop Dis. 28 déc 2015;9(12):e0004290.

780   46. Takougang I, Meli J, Wabo Poné J, Angwafo F. Community acceptability of the use of low-dose
781   niclosamide (Bayluscide®), as a molluscicide in the control of human schistosomiasis in Sahelian
782   Cameroon. Ann Trop Med Parasitol. 1 sept 2007;101(6):479-86.

783   47. Rohr JR, Sack A, Bakhoum S, Barrett CB, Lopez-Carr D, Chamberlin AJ, et al. A planetary health
784   innovation for disease, food and water challenges in Africa. Nature. juill 2023;619(7971):782-7.

785   48. Sokolow SH, Huttinger E, Jouanard N, Hsieh MH, Lafferty KD, Kuris AM, et al. Reduced
786   transmission of human schistosomiasis after restoration of a native river prawn that preys on the
787   snail intermediate host. Proc Natl Acad Sci. 4 août 2015;112(31):9650-5.

788   49. Sokolow SH, Wood CL, Jones IJ, Lafferty KD, Kuris AM, Hsieh MH, et al. To Reduce the Global
789   Burden of Human Schistosomiasis, Use 'Old Fashioned' Snail Control. Trends Parasitol. 1 janv
790   2018;34(1):23-40.

791   50. Selbach C, Mouritsen KN, Poulin R, Sures B, Smit NJ. Bridging the gap: aquatic parasites in the
792   One Health concept. Trends Parasitol. 1 févr 2022;38(2):109-11.

793

794

795   Figures in main text

796   Figure 1: Satellite map of the studied area in Northern Senegal.

797   This map indicates the location of the 9 targeted sites (black dots) and the name of the nearby 9

798   villages associated to these *S. haematobium* transmission sites.

799

800   Figure 2 : Co-infection ratio, *Schistosoma* prevalence, and *Schistosoma* cercariae ratio, for three values

801   of the carrying capacity.

802   The co-infection ratio is the ratio between the number of co-infected *B. truncatus* and the total number

803   of infected *B. truncatus*. The *Schistosoma* cercariae ratio is the ratio between the number of *Schistosoma*

804   cercariae and the total number of cercariae. The dashed purple line indicates the *Schistosoma* cercariae

805   ratio in case the *Schistosoma* shedding rate is the same as for the other trematode species. The reduction

806 of the *Schistosoma* cercariae ratio (difference between full and dashed purple line) is due to coinfections

807 and to the inferior competitivity of *Schistosoma*. The carrying capacity K differs by factors of 10 of the

808 snail population.

809

810 Figure 3: Relative abundance of trematode species in percentages of obtained sequenced reads

811 exploiting infected *B. truncatus* individual.

812 Infected snails (in columns) are grouped by site. The black dots correspond to the species of trematode

813 emitted by the emitting snails (confirmed by SANGER sequencing and BLAST assignation).

814

815

816 ## 7. Additional files

817 File name : Additional_File_1_(Figure_S1)

818 File format : .png

819 Title and description of the data : Equilibrium changes of density of miracidia, cercariae, susceptible

820 and infected snails, as a function of the carrying capacity (K) of the snail population in the case of one

821 trematode species infect the snail population.

822

823 File name : Additional_File_2_(Figure_S2)

824 File format : .png

825 Title and description of the data : Equilibrium changes of density of total miracidia and total cercariae

826 of two trematodes species including one with a lowest competitive capacity (i.e., *Schistosoma*), and of

827 density of susceptible and infected snails, as a function of the carrying capacity K of the snail population.

828

829 File name : Additional_File_3_(Figure_S3)

830 File format : .png

831 Title and description of the data : Equilibrium changes of co-infection ratio and *Schistosoma* cercariae

832 density ratio as a function of the carrying capacity (K) of the snail population in the case of two

833 trematodes species infecting the snail population. Note that without co-infection the ratio of *Schistosoma*

834   cercariae would be equal to 1/2. The deviation observed here is due to, and increases with, the co-

835   infection ratio.

836

837   File name : Additional_File_4_(Supplementary_material)

838   File format : .doc

839   Title and description of the data : Supplementary_material providing an in-depth description of the

840   model equations and simulations

841

842   File name : Additional_File_5_divpara_main.m

843   File format : MatLab (.m) https://fr.mathworks.com/products/matlab.html

844   Title and description of the data : MatLab script to generate Figure 2

845

846   File name : Additional_File_6_divpara_rhs.m

847   File format : MatLab (.m) https://fr.mathworks.com/products/matlab.html

848   Title and description of the data : MatLab functions to evaluate the right-hand side of the model

849   equations

850

851   File name : Additional_File_7_(Table S1)

852   File format : .xls

853   Title and description of the data : OTUs table assigned as trematodes of *B truncatus* from the

854   experimental infection positive to the trematode diagnostic

855

856   File name : Additional_File_8_(Figure_S4)

857   File format : .png

858   Title and description of the data : Number of *B. truncatus* individuals non infected, and infected by one

859   to 4 parasites species. Observed data are shown as bars. The negative binomial theoretical distribution

860   is represented by the black dots. The Chi2 test shows no statistical difference between the observed

861   distribution and the theoretical distribution suggesting a parasites aggregation in host populations (p-

862   value = 0.9985).

863

864   File name : Additional_File_9_(Table S2)

865   File format : .xls

866   Title and description of the data : OTUs assigned as trematodes found in water filtrations and in *B*

867   *truncatus* populations

868

869

870   File name : Additional_File_10_(Table S3)

871   File format : .xls

872   Title and description of the data : Prevalence of *Schistosoma* and trematodes in the different

873   populations of *B. truncatus*

874

875   File name : Additional_File_11_ (Figure S5)

876   File format : .png

877   Title and description of the data : Cercariae emission of *S. haematobium* or *S. bovis* as a function of

878   their relative abundance in case of co-infection with one or more other trematode species. Only *B.*

879   *truncatus* snails emitters infected by one species of *Schistosoma* and by at least one other species of

880   trematode were taken into account in this analysis (i.e. 14 snails). intra-mollusc parasitic stages and

881   cercariae of schistosomes are illustrated in red. Purple represents the intra-mollusc parasitic stages and

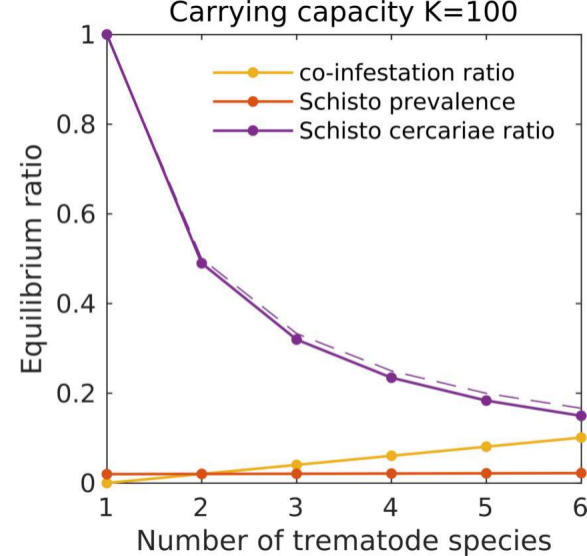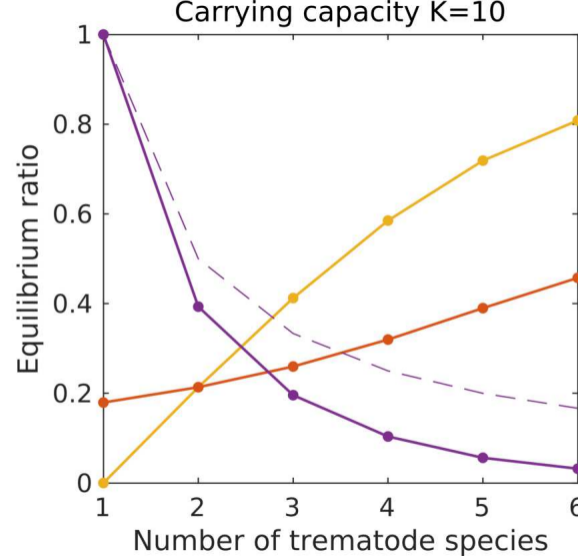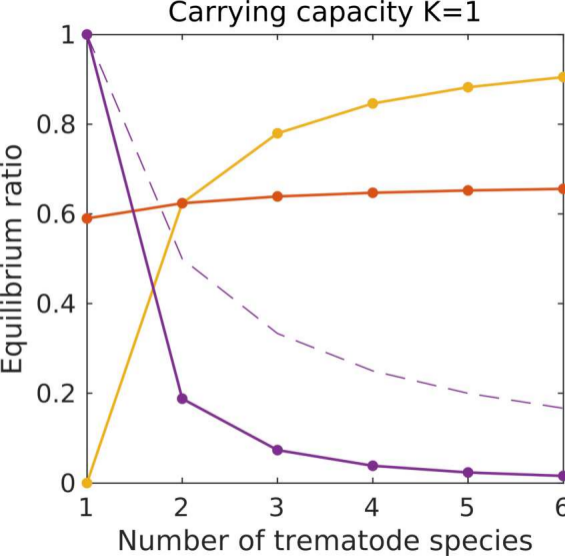882   cercariae of other co-infecting trematode species.
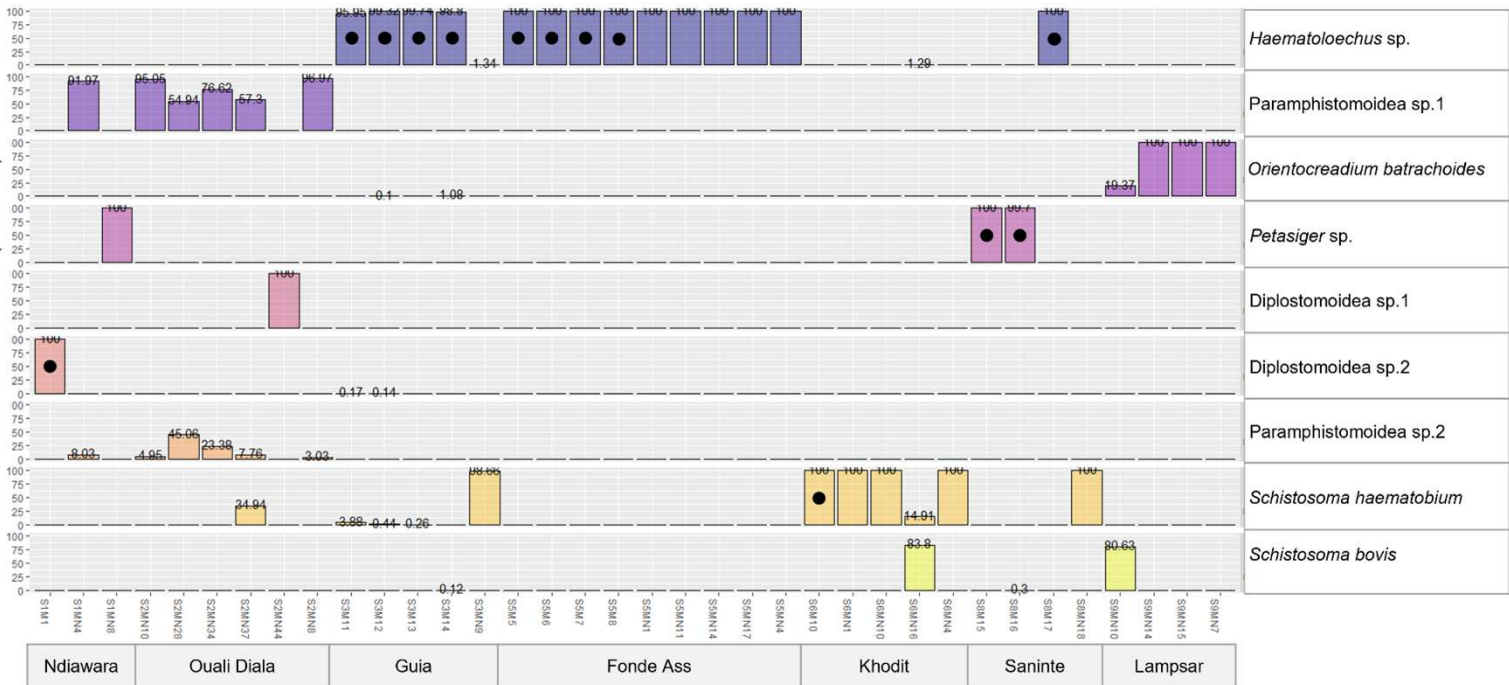
Supplementary Files

This is a list of supplementary files associated with this preprint. Click to download.

- AdditionalFile1FigureS1.png
- AdditionalFile2FigureS2.png
- AdditionalFile3FigureS3.png
- AdditionalFile4Supplementarymaterial.docx
- AdditionalFile5divparamain.m
- AdditionalFile6divpararhs.m
- AdditionalFile7TableS1.xlsx
- AdditionalFile8FigureS4.png
- AdditionalFile9TableS2.xlsx
- AdditionalFile10TableS3.xlsx
- AdditionalFile11FigureS5.png